G-to-A Hypermutation in Hepatitis B Virus (HBV) and Clinical Course of Patients with Chronic HBV Infection

Chiemi Noguchi,[1,2] Michio Imamura,[1,2] Masataka Tsuge,[1,2] Nobuhiko Hiraga,[1,2] Nami Mori,[1,2] Daiki Miki,[1,2] Takashi Kimura,[1,2] Shoichi Takahashi,[1,2] Yoshifumi Fujimoto,[1,2] Hidenori Ochi,[2,3] Hiromi Abe,[1,3] Toshiro Maekawa,[3] Chise Tateno,[2,4] Katsutoshi Yoshizato,[2,4] and Kazuaki Chayama[1,2,3]

[1]Department of Medicine and Molecular Science, Division of Frontier Medical Science, Programs for Biomedical Research, Graduate School of Biomedical Sciences, and [2]Liver Research Project Center, Hiroshima University, Hiroshima, [3]Laboratory for Liver Diseases, Single-Nucleotide Polymorphism Research Center, the Institute of Physical and Chemical Research, Yokohama, and [4]PhoenixBio, Higashihiroshima, Japan

Background. The apolipoprotein B messenger RNA editing enzyme, catalytic polypeptide–like family of cytidine deaminases induce G-to-A hypermutation in hepatitis B virus (HBV) genomes and play a role in innate antiviral immunity. The clinical relevance of this protein family is unknown.

Methods. We analyzed 33 instances in which 17 patients with chronic HBV infection experienced >2 increases of >100 IU/L in alanine aminotransferase (ALT) level; we used a quantitative differential DNA denaturation polymerase chain reaction assay to quantify the hypermutated HBV genomes observed during 21 of these 33 increases in ALT level.

Results. Of the 9 increases in ALT level that involved a >5-fold increase (relative to basal levels) in the number of hypermutated genomes observed, 8 were associated with a >2-log reduction in plasma HBV DNA level. In contrast, a corresponding decrease in plasma HBV DNA level was observed for only 1 of the 12 increases in ALT level that did not involve an increase in the number of hypermutated genomes ($P < .001$). Hepatitis B e antigen clearance was often observed in patients who experienced an increase in the number of hypermutated genomes. Interferon treatment induced hypermutation in HBV genomes in an animal model. However, there was no apparent increase in the number of hypermutated genomes among the majority of patients who received interferon therapy, probably because the number of hypermutated genomes had already increased prior to the initiation of therapy.

Conclusion. Our results suggest that a marked increase in the number of hypermutated genomes represents a strong immunological host response against the virus and is predictive of hepatitis B e antigen clearance and plasma HBV DNA level reduction.

Despite the availability of safe and effective vaccines for >2 decades, hepatitis B virus (HBV) infection is still a global health problem. Worldwide, >2 billion people are infected with HBV, and chronic HBV infection affects ~400 million people [1, 2]. It is estimated that >500,000 people die annually because of cirrhosis and/or hepatocellular carcinoma due to HBV infection [3].

Recent reports have shown that cellular cytosine deaminase (apolipoprotein B messenger RNA [mRNA] editing enzyme, catalytic polypeptide–like 3G [APOBEC3G]), packaged in human immunodeficiency virus type 1 (HIV-1), induces G-to-A hypermutation to a nascent reverse transcript of HIV-1 and reduces the infectivity of HIV, thus contributing in part to innate antiviral activity [4–8]. HIV-1 overcomes this innate defense barrier in T cells with HIV virion infectivity factor, a protein that specifically targets APOBEC3G to proteasomal degradation [9–12]. HIV-1 can infect resting CD4 T cells in lymphoid tissues but not those circulating in peripheral blood [13–16]. Resting CD4 T cells in peripheral blood are protected from HIV infection through the action of the deaminase-active

Received 30 August 2008; accepted 6 November 2008; electronically published 28 April 2009.

Potential conflicts of interest: none reported.

Financial support: Ministry of Education, Sports, Culture and Technology and Ministry of Health, Labor and Welfare (Grants-in-Aid for scientific research and development).

Reprints or correspondence: Kazuaki Chayama, MD, Dept. of Medical and Molecular Science, Div. of Frontier Medical Science, Programs for Biomedical Research, Graduate School of Biomedical Science, Hiroshima University, 1-2-3 Kasumi, Minami-ku, Hiroshima 734-8551, Japan (chayama@hiroshima-u.ac.jp).

The Journal of Infectious Diseases 2009; 199:1599–607

0022-1899/2009/19911-0007$15.00

DOI: 10.1086/598951

Table 1. Clinical profiles of 17 patients with chronic hepatitis B virus (HBV) infection who experienced >2 increases of >100 IU/L in alanine aminotransferase (ALT) level.

Patient	Sex	Age, years	ALT level, IU/L		Plasma HBV DNA level, log copies/mL	HBV serum marker status[a]		HBV subtype	Histologic result[b]	Receipt of IFN treatment
			Minimum	Maximum		HBeAg	HBeAb			
1	M	50	26	2000	8.1	+	−	C	F2, A2	Yes
2	M	31	22	230	8.2	+	−	C	F3, A2	Yes
3	F	23	14	313	8.7	+	−	C	F2, A2	Yes
4	M	22	16	846	6.9	+	−	C	F2, A1	Yes
5	F	42	10	100	7.8	+	−	C	L	No
6	F	33	21	748	8.8	+	−	C	F2, A3	Yes
7	M	23	22	339	8.4	+	−	C	L	Yes
8	F	54	22	108	6.7	−	+	C	F2, A2	No
9	M	44	17	512	9.5	+	−	C	F2, A3	No
10	M	27	39	115	8.8	+	−	C	F1, A1	Yes
11	M	36	16	452	3.8	+	−	C	F4, A3	Yes
12	M	20	21	1295	7.2	+	−	C	F2, A2	No
13	M	36	24	481	5.7	−	+	C	F2, A2	Yes
14	M	22	20	696	5.9	+	−	C	F1, A1	Yes
15	F	24	14	1544	7.7	+	−	C	F2, A2	Yes
16	M	35	10	1618	4.7	+	−	C	F2, A1	Yes
17	M	30	21	1655	6.7	+	−	C	L	Yes

NOTE. HBeAg, HBV e antigen; HBeAb, antibody against HBV e antigen; IFN, interferon; L, liver cirrhosis.

[a] Before increase in ALT level.

[b] Histologic evaluation of chronic hepatitis by use of the scoring system of Desmet et al. [29].

APOBEC3G [17]. Recent reports have shown that interferon (IFN)–α is a potent inducer of APOBEC3G [18–21]. It has also been reported that some of the HIV restriction exerted by APOBEC3G may be independent of its cytidine deaminase activity [17, 22–24].

We and others have reported the presence of small numbers of hypermutated genomes in serum samples obtained from HBV-infected patients [25–27]. Studies using HepG2 cell lines and primary human hepatocytes showed that such hypermutation is induced by the cytidine deaminase activity of the APOBEC family of proteins [27]. In our previous study, IFN induced little hypermutation in the HBV genome [27]. However, after extensive investigation supported by development of a quantitative analysis of hypermutation, we showed that both IFN-α and IFN-γ actually increase transcription of APOBEC3G mRNA in HepG2 cell lines and induce an increase in the number of hypermutated genomes [28]. We also showed that APOBEC3G induces hypermutation in HBV and reduces HBV replication levels in the absence of the deaminase activity. Thus, APOBEC3G has dual antiviral actions against HBV and is thought to be part of the host defense mechanisms, as has been shown for HIV infection. Although it is assumed that APOBEC3G is important in the host anti-HBV defense system, little is known about the clinical importance of this enzyme, because there are no methods available for the precise quantification of small amounts of hypermutated genomes.

Using a method that can measure small amounts of hypermutated genomes (differential DNA denaturation polymerase chain reaction [3D-PCR] combined with TaqMan PCR [28]), we analyzed fluctuations in the number of hypermutated genomes observed in patients with chronic HBV infection who experienced increased alanine aminotransferase (ALT) levels. The study group included patients who received IFN treatment and patients who did not.

METHODS

Patients. From 2002 through 2006 at Hiroshima University Hospital (Hiroshima, Japan), there were 17 consecutive patients with chronic hepatitis B who experienced >2 increases of >100 IU/L in ALT level and for whom stored serum samples were available. These 17 patients were enrolled in this study, among whom 33 such increases in ALT level were observed. Thirteen of 17 patients received IFN treatment, usually during an increase in ALT level. The clinical profiles of these 17 patients are shown in table 1. Written informed consent was obtained from all patients, and the study was approved by the Hiroshima University Ethics Committee.

HBV markers. Hepatitis B e antigen and antibody against e antigen were quantified by use of enzyme immunoassay kits (Abbott Diagnostics). HBV DNA was measured by use of real-time PCR performed with the 7300 Real-Time PCR System (Applied Biosystems), in accordance with the manufacturer's instructions. The primers used for amplification were 5'-TT-

TGGGCATGGACATTGAC-3' (nt 1893–1912; nucleotide numbers are those of HBV subtype C as reported by Norder et al. [30]) and 5'-GGTGAACAATGTTCCGGAGAC-3' (nt 2029–2049). For real-time PCR, we used 25 μL of SYBR Green PCR Master Mix (Applied Biosystems) with 1 μL of the DNA solution and 200 nmol/L of each primer. The amplification conditions were as follows: 2 min at 50°C, 10 min at 95°C, followed by 40 cycles of amplification (denaturation at 95°C for 15 s and annealing and extension at 60°C for 1 min). The lower detection limit of this assay was 10^3 copies/mL.

Extraction of HBV DNA and quantitative analysis of hypermutated genomes. HBV DNA was extracted from 100-μL serum samples by use of the SMITEST DNA Extraction Kit (Genome Science Laboratories) and dissolved in 20 μL of water. Hypermutated genomes were quantified by use of TaqMan 3D-PCR performed with the 7300 Real-Time PCR System (Applied Biosystems); we used a procedure described elsewhere [28], with slight modifications. In brief, the HBV DNA fragments were amplified by use of 3D-PCR in which the denaturation temperature was set lower than usual so that only G-to-A hypermutated genomes would be amplified. The amplification conditions were as follows: activation at 95°C for 10 min; followed by initial denaturation at 89°C for 20 min, to allow nonhypermutated genomes reanneal; and 45 cycles of amplification (denaturation at 89°C for 20 s, annealing at 50°C for 30 s, and extension at 62°C for 90 s). TaqMan PCR was performed using the following primers: 5'-ACTTCAACCCCAACAMRRATCA-3' (nt 2978–2999) and 5'-AGAGYTTGKTGGAATGTKGTGGA-3' (nt 24–1), where M is A or C, R is G or A, Y is T or C, and K is G or T. The probe was a 6-carboxyfluorescein (FAM)–labeled MGB probe, 5'-(FAM)-TTAGAGGTGGAGAGATGG-(MGB)-3' (nt 3184–3167). The detection limit of hypermutated genomes was 10^2 copies/mL, and nonhypermutated genomes were not amplified by 3D-PCR [28]. The reproducibility of the assay was quite high (as indicated by the small standard deviation relative to the results of the quantitative PCR control reaction), as reported in our previous study [28].

Cell culture and transfection. HepG2 cell lines were grown in Dulbecco's modified Eagle medium supplemented with 10% (vol/vol) fetal calf serum at 37°C in 5% CO_2. Cells were seeded to semiconfluence in 6-well tissue culture plates and transfected with the plasmid pTRE-HB-wt, which contained 1.4–genome length wild-type HBV genomes [31], by calcium phosphate precipitation. Seventy-two hours after transfection, the supernatant was collected for HBV DNA quantification by real-time PCR and for quantitative analysis of G-to-A hypermutated genomes [28]. The remaining supernatant was stored at −80°C for infection experiments using human hepatocyte–chimeric mice.

Quantitative analysis of G-to-A hypermutated genomes with human hepatocyte–chimeric mice. A human hepatocyte–chimeric mouse model was developed, as described previously [32], and used in infection and IFN-treatment experiments. The human hepatocytes progressively repopulated the murine host liver and were susceptible to HBV produced in cultured cell lines [31]. All animal protocols were in accordance with the guidelines of the local animal experimentation committee. The experimental protocol was approved by the Ethics Review Committee for Animal Experimentation of the Graduate School of Biomedical Sciences, Hiroshima University. Hepatocyte-chimeric mice were inoculated with 500 μL of the supernatant produced by transiently transfected cell lines. After confirmation of high-level HBV viremia, the mice were treated with 7000 IU/g/day of IFN-α, injected intramuscularly, for 14 days (the IFN-α was a gift from Hayashibara Biochemical Labs in Okayama, Japan). Human serum albumin in mouse serum was measured with the Human Albumin ELISA Quantitation Kit (Bethyl Laboratories), used in accordance with the manufacturer's instructions.

Statistical analysis. Differences between clinical groups with respect to HBV DNA and e antigen levels were examined for statistical significance, using the Mann-Whitney *U* test. A *P* value $<.05$ was considered to indicate a statistically significant difference. All statistical analyses were performed with StatView (version 5.0; SAS Institute).

RESULTS

Clinical course of disease in patients with increased ALT levels and fluctuations in the number of hypermutated genomes. Figure 1*A*–1*D* shows clinical courses for 4 representative patients (patients 1–4 in Table 1) with chronic HBV infection who experienced increases in ALT level. We observed marked decreases in HBV DNA level in association with marked increases in hypermutated genomes (figure 1*A*–1*C*, black arrows). In contrast, there was no apparent reduction in HBV level in the absence of an increase in hypermutated genomes (1*A*–1*D*, white arrows). We also analyzed the effect of IFN therapy on the number of hypermutated genomes. In some patients, we observed an increase in the number of hypermutated genomes during IFN therapy (figure 1*B* and 1*C*) as well as a marked increase in the number of hypermutated genomes and a reduction of the virus accompanied by an increase in ALT level just after cessation of IFN therapy (1*A*–1*C*, black arrows). However, in some patients, such as patient 1 (figure 1*A*), we observed no apparent increase in the number of hypermutated genomes in response to IFN therapy. However, the number of hypermutated genomes observed in samples from this patient obtained just before the initiation of IFN therapy (996/10^6 genomes) was already higher than the baseline level (157/10^6 genomes). Samples from patient 4 (figure 1*D*) showed an increase in the number of hypermutated genomes during IFN therapy (1907/10^6 genomes), though this is less than the increase observed during natural exacerbation (12,404/10^6 genomes). In fact, there was no significant difference between IFN-treated patients and untreated patients with respect to the number of hypermutated genomes observed (data not shown). These results suggest that the host's antiviral immunity level was higher at baseline than it was after

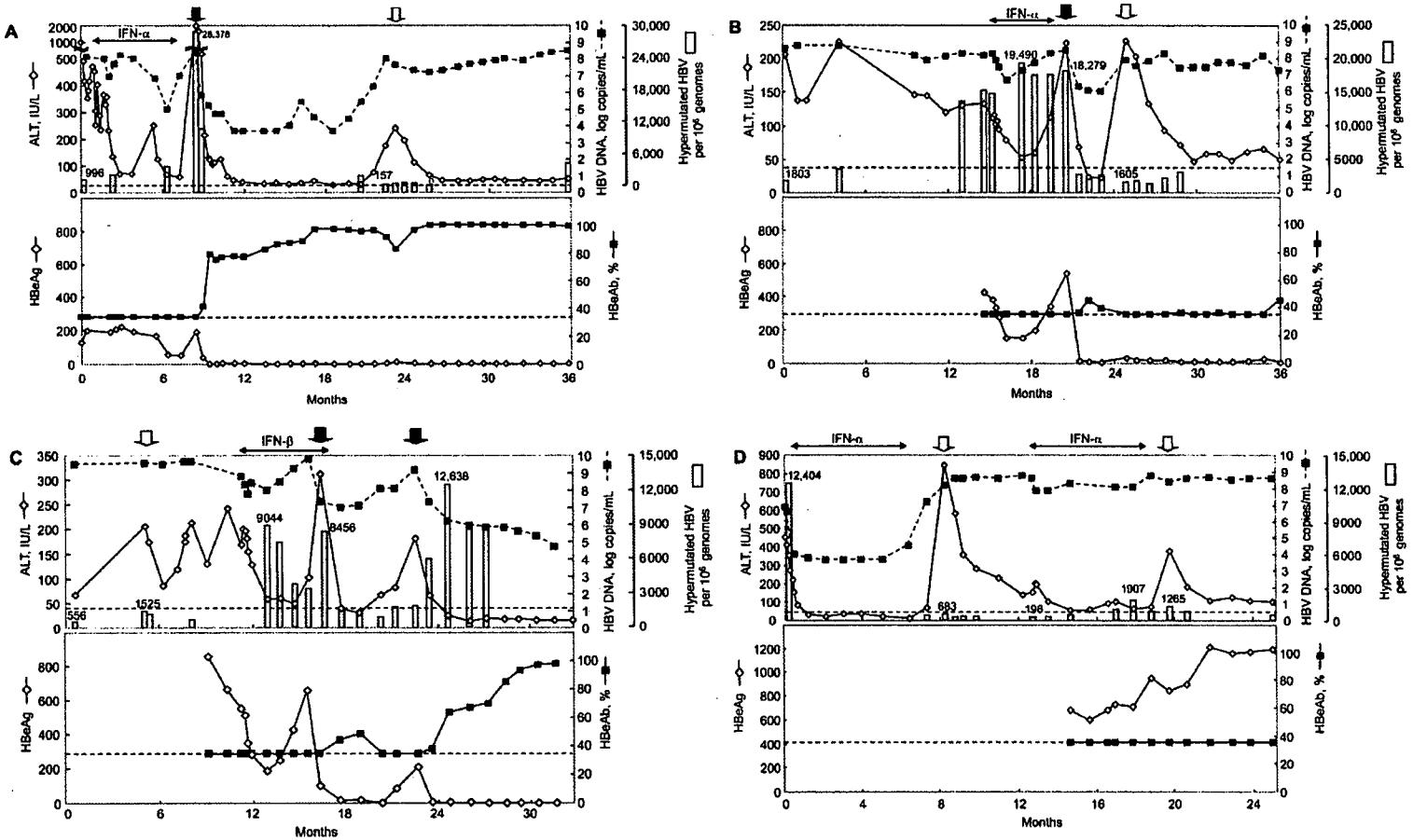

Figure 1. Clinical courses for 4 patients *(A–D)* with chronic hepatitis B virus (HBV) infection who experienced exacerbation of infection. *Black arrows,* exacerbation associated with an increase in the number of hypermutated genomes (>5 times basal levels); *white arrows,* exacerbation not associated with an increase in the number of hypermutated genomes; *horizontal dotted lines,* upper normal limit of alanine aminotransferase (ALT) (40 IU/mL; *upper panel, A–D*) and the detection limit for antibody against e antigen (HBeAb) (35%; *lower panel, A–D*). HBeAb, antibody against HBV e antigen; HBeAg, HBV e antigen; IFN, interferon.

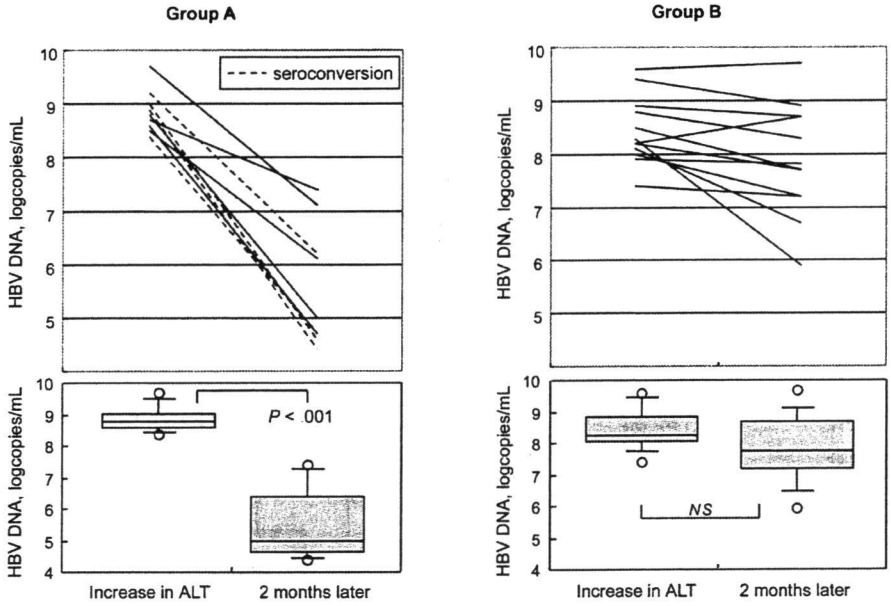

Figure 2. Relationship between increase in the number of hypermutated genomes and plasma levels of hepatitis B virus (HBV) DNA in 17 patients with chronic HBV infection who experienced >2 increases of >100 IU/L in alanine aminotransferase (ALT) level. Patients' exacerbations were divided into 2 groups, A and B, according to the extent of increase in the number of hypermutated genomes, relative to the basal number (group A included 9 exacerbations that involved a >5-fold increase in the number of hypermutated genomes; group B included 12 exacerbations that involved a ≤5-fold increase in the number of hypermutated genomes). *Upper panel* for groups A and B, individual HBV DNA levels at the time the ALT level increased and 2 months later; in the upper panel for group A, *dashed lines* indicate 4 exacerbations associated with seroconversion to positivity for antibody against e antigen. *Lower panel* for groups A and B, box-and-whisker plots for HBV DNA levels at same 2 time points. In the plots, the lines in the boxes indicate median values; the upper and lower lines of the boxes indicate the 25th and 75th percentiles, respectively; and the upper and lower whiskers represent the 90th and 10th percentiles, respectively.

IFN or that the feedback system for IFN signaling was already active before initiation of therapy.

We also compared the degree of reduction in the plasma HBV DNA level for exacerbations (i.e., increases in ALT level) associated with a marked increase in the number of hypermutated genomes (i.e., those in which the peak number was >5 times the number observed prior to exacerbation) and for exacerbations not associated with such an increase. As shown in figure 2, 8 of 9 exacerbations that were coupled with a marked increase in the number of hypermutated genomes (group A) were associated with a >2-log reduction in the HBV DNA level. In contrast, only 1 of the 12 exacerbations not associated with a marked increase in the number of hypermutated genomes (group B) was associated with a >2-log reduction in plasma HBV DNA level. The median serum HBV DNA level decreased from 8.8 to 5.0 log copies/mL among the patients in group A ($P < .001$) but did not decrease for patients in group B (figure 2).

In addition, we compared the reduction in e antigen level for these 2 groups. Levels were reduced in both groups, but the median reduction was more prominent for patients in group A than for those in group B (figure 3). All 4 exacerbations coupled with e antigen seroconversion (from positive to negative) were associated with marked increase in hypermutated genomes (figure 3).

Effect of IFN treatment on the rate of HBV hypermutation in chimeric mice. Next, we examined the effect of IFN treatment on G-to-A hypermutation in HBV genomes in human hepatocyte–chimeric mice. Two mice were intravenously injected with supernatant produced by HepG2 cells transiently transfected with a plasmid containing 1.4–genome length wild-type HBV genomes. Ten weeks later, after confirmation of high-level HBV viremia, the mice were treated with 7000 IU/g/day of IFN-α, injected intramuscularly, for 14 days. We observed an ~1.5-log reduction in plasma HBV DNA level accompanied by an increase in the number of hypermutated genomes in both mice (figure 4*A*). In a mouse inoculated with HBV but treated with phosphate-buffered saline, no increase of hypermutated genomes was observed (figure 4*B*). We also observed a 36-fold increase in the level of APOBEC3G mRNA, as determined by human oligonucleotide microarray (data not shown).

Infectivity of hypermutated genomes. To study the biological significance of hypermutated genomes, culture supernatant from HepG2 cells transfected with both HBV and APOBEC3G (5 μg each) was injected into a chimeric mouse. As shown in figure 5, the culture supernatant contained a large number of hypermutated genomes. In contrast, we could not detect hypermutated genomes in the chimeric mouse inoculated with this

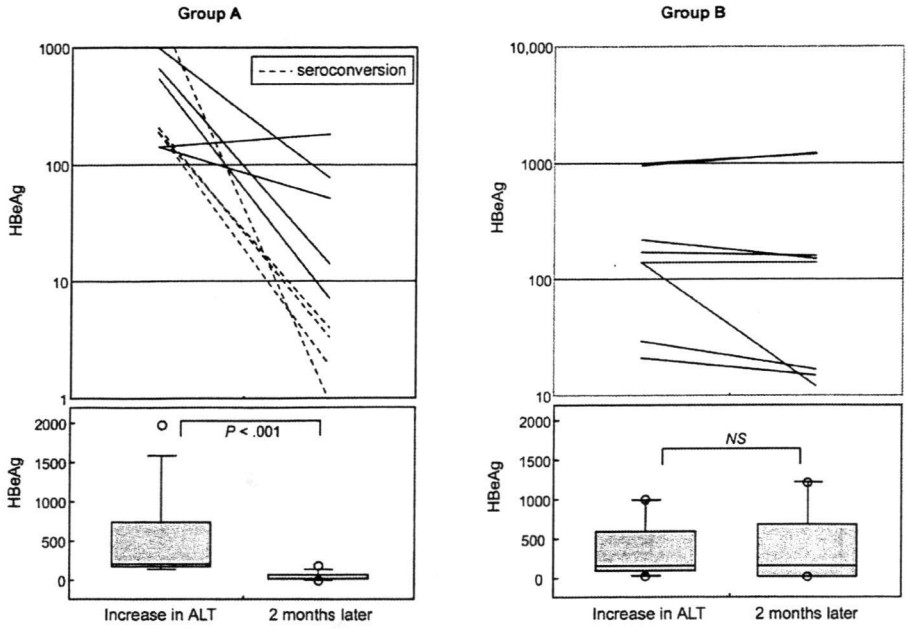

Figure 3. Relationship between increase in the number of hypermutated genomes and hepatitis B virus (HBV) e antigen (HBeAg) levels in 15 HBeAg-positive patients with chronic HBV infection who experienced >2 increases of >100 IU/L in alanine aminotransferase (ALT) level. Patients' exacerbations were divided into 2 groups, A and B, according to the extent of increase in the number of hypermutated genomes, relative to the basal number (group A included 9 exacerbations that involved a >5-fold increase in the number of hypermutated genomes; group B included 8 exacerbations that involved a ≤5-fold increase in the number of hypermutated genomes). *Upper panel* for groups A and B, individual e antigen levels at the time the ALT level increased and 2 months later; in the upper panel for group A, *dashed lines* indicate 4 exacerbations associated with seroconversion to positivity for antibody against e antigen. *Lower panel* for groups A and B, box-and-whisker plots for e antigen levels at these same 2 time points. In the plots, the lines in the boxes indicate median values; the upper and lower lines of the boxes indicate the 25th and 75th percentiles, respectively; and the upper and lower whiskers represent the 90th and 10th percentiles, respectively.

supernatant (figure 5*A* and 5*B*). These results suggest that the infectivity (or replication ability) of HBV with hypermutated genomes is very poor. It is possible that the inoculum contained less abundantly mutated genomes. To test this, we cloned and sequenced 72 clones of 217-bp DNA fragments amplified at a denaturation temperature of 95°C. Of 72 clones obtained from the inoculum, we found 1 clone with 8 G-to-A substitutions, 1 clone with 5 substitutions, 2 clones with 3 substitutions, and 1 clone with 1 substitution (figure 5*C*). In contrast, 1 of the 72 clones obtained from the mouse serum had 1 G-to-A substitution. If G-to-A substitutions were excluded, the only other nucleotide substitution observed in the 144 clones sequenced was a single C-to-T substitution.

DISCUSSION

In a previous study, we found that the majority of serum samples obtained from HBV-infected patients contained a small number of hypermutated genomes [27]. Recently, we developed a method (TaqMan 3D-PCR) to measure small numbers of hypermutated genomes [28]. Using this method, we reported dual antiviral effects for APOBEC3G, namely induction of hypermutation and reduction of viral replication. We also reported that IFN increased the transcription of APOBEC3G and enhanced the effect of the protein in vitro [28]. Other investigators also showed that IFN enhances the action of APOBEC proteins against HIV [18–21]. It is thus assumed that the antiviral effect of APOBEC proteins should be enhanced by IFN and other cytokines in vivo.

In the present study, we showed that an increase in ALT level accompanied by an increase in the number of hypermutated genomes was associated with reduction in the plasma HBV DNA level. In contrast, no decrease in HBV DNA level was observed if the increase in ALT level occurred in the absence of an increase in the number of hypermutated genomes. It is difficult to know which of the dual antiviral effects of APOBEC3G (or other APOBEC proteins) reduced the viral level. It is also impossible to estimate the importance of APOBEC proteins in this reduction. However, it is clear that the increase in the number of hypermutated genomes of HBV correlates with activation of the host antiviral defense against HBV.

We also demonstrated that exacerbations of HBV infection associated with a marked increase in the number of hypermutated genomes were associated not only with a decrease in the plasma HBV DNA level but also with clearance of e antigen.

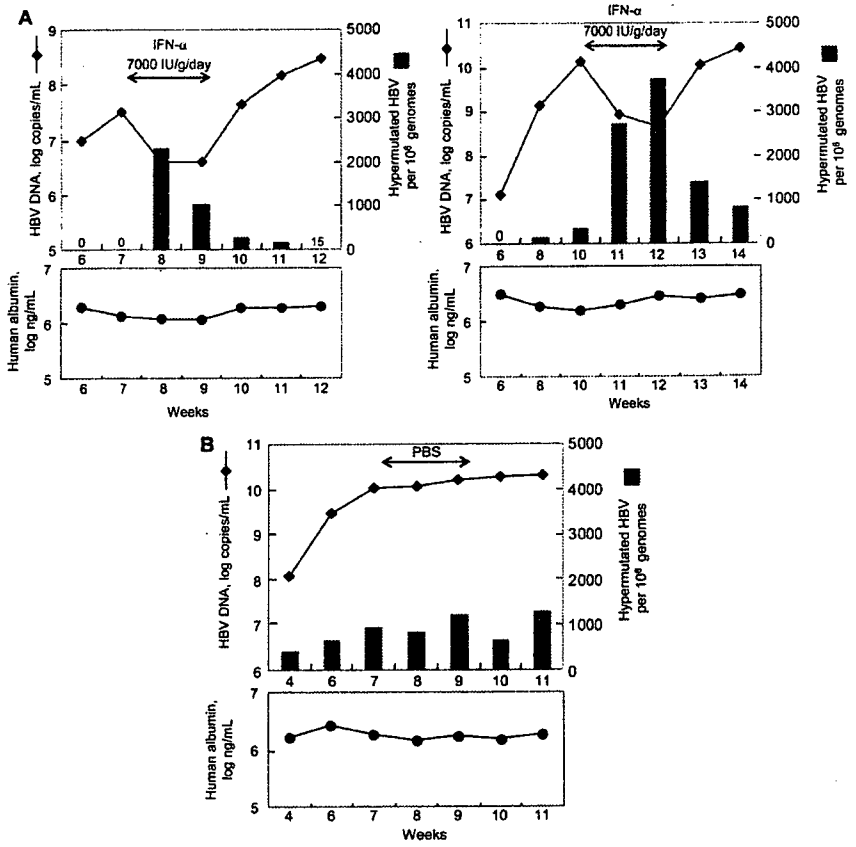

Figure 4. Effect of interferon (IFN)–α therapy on hepatitis B virus (HBV) hypermutation in HBV-infected, human hepatocyte–chimeric mice. Two chimeric mice *(A)* were inoculated with recombinant wild-type HBV produced by transfected HepG2 cells; 10 weeks later, after confirmation of high-level HBV viremia, they were treated with IFN-α at 7000 IU/g/day for 14 days, by intramuscular injection. *Upper panels* in both parts of *A*, serum HBV DNA levels and the number of hypermutated genomes; *lower panels* in both parts of *A*, human serum albumin concentrations. Note that the albumin levels are stable during IFN-α therapy. A control mouse *(B)* was inoculated with recombinant wild-type HBV produced by transfected HepG2 cells and treated with phosphate-buffered saline (PBS). Upper and lower panels of *B* show the same information as in *A*.

Furthermore, all exacerbations followed by seroconversion to positivity for antibody against e antigen were associated with a marked increase in the number of hypermutated genomes. Clearance of e antigen often results from a G-to-A nucleotide substitution at the first position of a 5'-GGGG stretch in the precore coding sequence (the G1896A mutation). Because this substitution (changing TGGGG to TAGGG) is in agreement with the dinucleotide pattern preferentially edited by APOBEC3G, one might assume that G-to-A substitution in this region could be caused by this enzyme and is related to the clearance of e antigen. However, we observed that hypermutation was induced in only some genomes, whereas the majority of genomes were unaffected. Thus, it seems unlikely that APOBEC proteins play a role in seroconversion to positivity for antibody against e antigen, although it is still possible that the 5'-GGGG stretch in the precore region is the preferred editing site for the enzyme. Importantly, such substitution of the 5'-GGGG stretch should result in the occurrence of multiple stop codons (TAG, TGA, and TAA) in HBV genomes, as we observed and reported in our previous study [28], which makes the replication of mutated genomes impossible.

In the present study, we did not observe any increase in the number of hypermutated genomes during IFN therapy in some patients. This finding is discrepant from the results of previous in vitro experiments that showed increased numbers of hypermutated genomes after the application of IFN [28]. Interestingly, our experimental results also showed the induction of APOBEC3G gene expression, an increase in the number of hypermutated genomes, and a reduction of plasma HBV DNA level in 2 human hepatocyte–chimeric mice treated with IFN (figure 4). What is the reason for the lack of increase in hypermutation in some IFN-treated patients? We usually administer IFN to patients who have high ALT levels. The patients in this study had abnormal ALT levels prior to treatment with IFN—that is, their livers were inflamed, and the levels of many cytokines produced by the immune cells in the liver were already high. We presume that the effect of these elevated cytokine levels masked the effect of the IFN we administered. It could also be argued that the effect

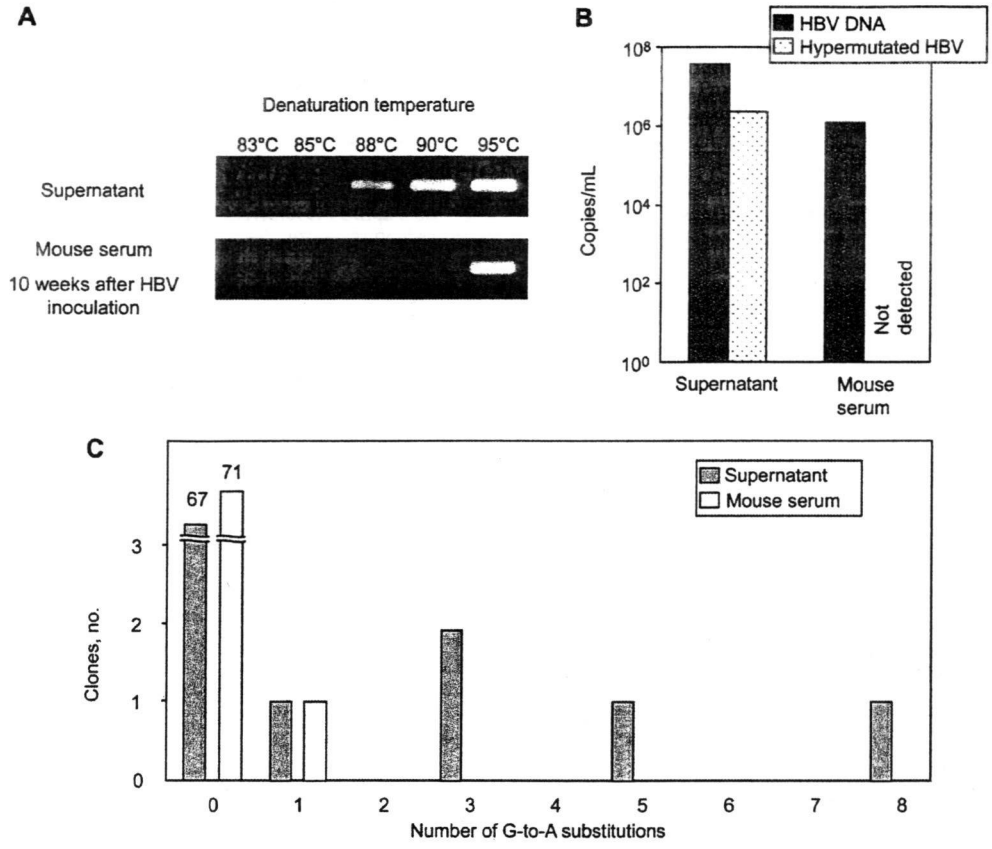

Figure 5. Results for a human hepatocyte–chimeric mouse inoculated with hepatitis B virus (HBV) produced by HepG2 cells transfected with an equal amount (5 μg each) of HBV and apolipoprotein B messenger RNA editing enzyme, catalytic polypeptide–like 3G plasmids. The inoculum contained ~6.25% hypermutated genomes. A serum sample was obtained 10 weeks after the inoculation. *A,* HBV DNA was amplified by polymerase chain reaction (PCR) that used different denaturation temperatures and run on 2% agarose gel. *B,* Quantitative measurement of HBV DNA and hypermutated DNA in the inoculum and mouse serum. *C,* Number of G-to-A substitutions found in each of 72 clones obtained from products of PCR of culture supernatant or mouse serum.

observed in mice represents the absence of the immune response in mice, whereas the lack of a clear response to IFN in the study patients was the result of the complex immune response in human beings. Alternatively, the concentrations of IFN in treated patients might be lower than those used for the cell culture or the chimeric mice. Although we did not perform this analysis in the present study, it would be interesting to determine the expression levels of APOBEC proteins and IFN-stimulated genes in the liver of IFN-treated patients.

The present study showed that the number of hypermutated genomes increased during some increases in ALT level, probably as a result of IFN-activated APOBEC proteins and other cytokines in patients with chronic hepatitis B. However, the number of hypermutated genomes was very small, only 28,378 in 10^6 HBV genomes at most (figure 1*A*). Because it was possible that the less abundantly hypermutated genomes were not detected (i.e., that genomes with only 1 or 2 G-to-A substitutions were not amplified by 3D-PCR), cloning and sequencing were performed to detect such genomes. However, the number of genomes containing G-to-A substitutions was still low (5 [6.9%] of 72 clones), even in the culture medium of HepG2 cells cotransfected with APOBEC3G and HBV (figure 5*C*). This means that the number of genomes with only a small number of G-to-A substitution was not high, suggesting that only selected DNA molecules were heavily mutated while the remaining DNA was not. Does this mean that the effect of APOBEC proteins in antiviral defense is trivial in patients with chronic HBV infection? It is a possible that the heavily deaminated genomes are an easy target for uracil DNA glycocylase. Although the dual antiviral effects of APOBEC proteins are currently known to reduce the amount of HBV, the importance and magnitude of APOBEC proteins with respect to in vivo virus reduction should be investigated further.

Treatment of patients with chronic HBV infection has improved with the advent of new nucleoside and nucleotide analogues. However, reactivation of HBV and flare-ups of hepatitis are often seen in patients who stop such therapy. Furthermore, hepatitis B surface antigen clearance is rare in patients treated

with these antiviral drugs. On the other hand, most patients with chronic HBV infection achieve sufficient viral suppression and disease quiescence through immunological suppression of the virus. As we showed in this study, the immunological suppression of HBV is much stronger than that achieved with IFN therapy, but it is often transient. It is thus necessary to clarify the mechanism of transient immune response and to develop treatment that produces persistent suppression of HBV. Quantitative measurement of hypermutated genomes should be useful in monitoring the immune response in this context.

Acknowledgments

We thank Rie Akiyama, Miyuki Matsushita, and Yoshiko Seo for excellent technical assistance and Yoshiko Nakata for secretarial assistance.

References

1. Wright TL, Lau JYN. Clinical aspects of hepatitis B virus infection. Lancet **1993**; 342:1340–4.
2. Ganem D, Prince AM. Hepatitis B virus infection: natural history and clinical consequences. N Engl J Med **2004**; 350:1118–29.
3. Bruix J, Llovet JM. Hepatitis B virus and hepatocellular carcinoma. J Hepatol **2003**; 39(Suppl 1):S59–63.
4. Sheehy AM, Gaddis NC, Choi JD, Malim MH. Isolation of a human gene that inhibits HIV-1 infection and is suppressed by the viral Vif protein. Nature **2002**; 418:646–50.
5. Mangeat B, Turelli P, Caron G, Friedli M, Perrin L, Trono D. Broad antiretroviral defence by human APOBEC3G through lethal editing of nascent reverse transcripts. Nature **2003**; 424:99–103.
6. Zhang HYB, Pomerantz RJ, Zhang C, Arunachalam SC, Gao L. The cytidine deaminase CEM15 induces hypermutation in newly synthesized HIV-1 DNA. Nature **2003**; 424:94–8.
7. Lecossier D, Bouchonnet F, Clavel F, Hance AJ. Hypermutation of HIV-1 DNA in the absence of the Vif protein. Science **2003**; 300:1112.
8. Harris RS, Bishop KN, Sheehy AM, et al. DNA determination mediates innate immunity to retroviral infection. Cell **2003**; 113:803–9.
9. Liu B, Yu X, Luo K, Yu Y, Yu XF. Influence of primate lentiviral vif and proteasome inhibitors on human immunodeficiency virus type 1 virion packaging of APOBEC3G. J Virol **2004**; 78:2072–81.
10. Mehle A, Strack B, Ancuta P, Zhang C, McPike M, Gabuzda D. Vif overcomes the innate antiviral activity of APOBEC3G by promoting its degradation in the ubiquitin-proteasome pathway. J Biol Chem **2004**; 279:7792–8.
11. Marin M, Rose KM, Kozak SL, Kabat D. HIV-1 Vif protein binds the editing enzyme APOBEC3G and induces its degradation. Nat Med **2003**; 9:1398–403.
12. Stopak K, de Noronha C, Yonemoto W, Greene WC. HIV-1 Vif blocks the antiviral activity of APOBEC3G by impairing both its translation and intracellular stability. Mol Cell **2003**; 12:591–601.
13. Zack JA, Arrigo SJ, Weitsman SR, Go AS, Haislip A, Chen IS. HIV-1 entry into quiescent primary lymphocytes: molecular analysis reveals a labile, latent viral structure. Cell **1990**; 61:213–22.
14. Korin YD, Zack JA. Progression to the G1b phase of the cell cycle is required for completion of human immunodeficiency virus type 1 reverse transcription in T cells. J Virol **1998**; 72:3161–8.
15. Pierson TC, Zhou Y, Kieffer TL, Ruff CT, Buck C, Siliciano RF. Molecular characterization of preintegration latency in human immunodeficiency virus type 1 infection. J Virol **2002**; 76:8518–31.
16. Stevenson M, Stanwick TL, Dempsey MP, Lamonica CA. HIV-1 replication is controlled at the level of T cell activation and proviral integration. EMBO J **1990**; 9:1551–60.
17. Chiu YL, Soros VB, Kreisberg JF, Stopak K, Yonemoto W, Greene WC. Cellular APOBEC3G restricts HIV-1 infection in resting $CD4^+$ T cells. Nature **2005**; 435:108–14.
18. Tanaka Y, Marusawa H, Seno H, et al. Antiviral protein APOBEC3G is induced by interferon-alpha stimulation in human hepatocytes. Biochem Biophys Res Commun **2006**; 341:314–9.
19. Peng G, Lei KJ, Jin W, Greenwell-Wild T, Wahl SM. Induction of APOBEC3 family proteins, a defensive maneuver underlying interferon-induced anti-HIV-1 activity. J Exp Med **2006**; 203:41–6.
20. Bonvin M, Achermann F, Greeve I, et al. Interferon-inducible expression of APOBEC3 editing enzymes in human hepatocytes and inhibition of hepatitis B virus replication. Hepatology **2006**; 43:1364–74.
21. Chen K, Huang J, Zhang C, et al. Alpha interferon potently enhances the anti-human immunodeficiency virus type 1 activity of APOBEC3G in resting primary CD4 T cells. J Virol **2006**; 80:7645–57.
22. Newman EN, Holmes RK, Craig HM, et al. Antiviral function of APOBEC3G can be dissociated from cytidine deaminase activity. Curr Biol **2005**; 15:166–70.
23. Navarro F, Bollman B, Chen H, et al. Complementary function of the two catalytic domains of APOBEC3G. Virology **2005**; 333:374–86.
24. Nguyen DH, Gummuluru S, Hu J. Deamination-independent inhibition of hepatitis B virus reverse transcription by APOBEC3G. J Virol **2007**; 81:4465–72.
25. Gunther S, Sommer G, Plikat U, Iwanska A, WainHobson S, Will H, et al. Naturally occurring hepatitis B virus genomes bearing the hallmarks of retroviral G→A hypermutation. Virology **1997**; 235:104–8.
26. Suspene R, Guetard D, Henry M, Sommer P, Wain-Hobson S, Vartanian JP. Extensive editing of both hepatitis B virus DNA strands by APOBEC3 cytidine deaminases in vitro and in vivo. Proc Natl Acad Sci U S A **2005**; 102:8321–6.
27. Noguchi C, Ishino H, Tsuge M, et al. G to A hypermutation of hepatitis B virus. Hepatology **2005**; 41:626–33.
28. Noguchi C, Hiraga N, Mori N, et al. Dual effect of APOBEC3G on hepatitis B virus. J Gen Virol **2007**; 88:432–40.
29. Desmet VJ, Gerber M, Hoofnagle JH, Manns M, Scheuer PJ. Classification of chronic hepatitis: diagnosis, grading and staging. Hepatology **1994**; 19:1513–20.
30. Norder H, Courouce AM, Magnius LO. Complete genomes, phylogenetic relatedness, and structural proteins of 6 strains of the hepatitis-B virus, 4 of which represent 2 new genotypes. Virology **1994**; 198:489–503.
31. Tsuge M, Hiraga N, Takaishi H, et al. Infection of human hepatocyte chimeric mouse with genetically engineered hepatitis B virus. Hepatology **2005**; 42:1046–54.
32. Tateno C, Yoshizane Y, Saito N, et al. Near completely humanized liver in mice shows human-type metabolic responses to drugs. Am J Pathol **2004**; 165:901–12.

ELSEVIER

Journal of Hepatology 50 (2009) 1226–1235

Journal of Hepatology

www.elsevier.com/locate/jhep

Deletion of angiotensin II type I receptor reduces hepatic steatosis☆

Yoshitaka Nabeshima[1], Susumu Tazuma[2], Keishi Kanno[2,*], Hideyuki Hyogo[1], Kazuaki Chayama[1]

[1]*Department of Medicine and Molecular Science, Graduate School of Biomedical Sciences, Hiroshima University, Hiroshima, Japan*
[2]*Department of General Medicine, Hiroshima University Hospital, 1-2-3, Kasumi, Minami-ku, Hiroshima 734-8551, Japan*

***Background/Aims*: A distinct subgroup of angiotensin II type 1 receptor (AT1R) blockers (ARBs) have been reported to suppress the development of hepatic steatosis. These effects were generally explained by selective peroxisome proliferator-activated receptor (PPAR) γ modulating properties of ARBs, independent of their AT1R blocking actions. Here, we provide genetic evidence of the direct role for AT1R in hepatic steatosis.**

***Methods*: The effect of AT1R deletion on steatohepatitis was investigated in $AT1a^{-/-}$ mice. Furthermore, the influence of AT1R inhibition by telmisartan as well as gene silencing of AT1R by siRNA was assessed in an *in vitro* experiment using HepG2 cells.**

***Results*: Compared to wild-type (WT), $AT1a^{-/-}$ mice fed methionine–choline deficient (MCD) diet resulted in negligible lipid accumulation in the liver with marked induction of PPARα mRNA. *In vitro* experiments also demonstrated reduced cellular lipid accumulation by telmisartan and AT1R knockdown following exposure of long chain fatty acids. This is presumably explained by the observation that the expression of PPARα and its target genes were significantly up-regulated in specific siRNA treated HepG2 cells.**

***Conclusions*: Our data indicate, in addition to pharmacological effect of ARBs on PPARγ activation, a key biological role for AT1R in the regulation of hepatic lipid metabolism.**

***Keywords*: Lipid metabolism; Renin-angiotensin system; Non-alcoholic fatty liver disease; Non-alcoholic steatohepatitis; Peroxisome proliferator-activated receptor α**

1. Introduction

Non-alcoholic fatty liver disease (NAFLD) encompasses a wide spectrum of liver pathology – from simple steatosis alone, through necroinflammatory disorder referred to as non-alcoholic steatohepatitis (NASH), to cirrhosis and liver cancer. Because of the high prevalence and the potential mortality, NAFLD/NASH has emerged as a serious public concern and therefore therapeutic strategies need to be established. Recent animal studies and clinical trials have demonstrated several pharmacological treatments as potential therapeutic targets, which include insulin sensitizers (e.g., thiazolidinediones, metoformin), lipid lowering agents (e.g., statins, fibrates), antioxidants, angiotensin (Ang) II type I receptor (AT1R) blockers (ARBs), etc. [1–7]. Among

Received 16 September 2008; received in revised form 16 December 2008; accepted 9 January 2009; available online 11 March 2009
Associate Editor: C.P. Day

☆ The authors who have taken part in this study declared that they do not have anything to disclose regarding funding or conflict of interest with respect to this manuscript.

* Corresponding author. Tel./fax: +81 82 257 5461.
E-mail address: kkanno@hiroshima-u.ac.jp (K. Kanno).

Abbreviations: AT1R, angiotensin II type 1 receptor; ARB, angiotensin II type 1 receptor blocker; PPAR, peroxisome proliferator-activated receptor; Ang, angiotensin; WT, wild-type; MCD, methionine–choline deficient; TBARS, thiobarbituric acid-reactive substances; TG, triglyceride; NAFLD, nonalcoholic fatty liver disease; NASH, nonalcoholic steatohepatitis; HSC, hepatic stellate cell; siRNA, small interfering RNA; DMSO, dimethyl sulfoxide; FFA, free fatty acid; PBS, phosphate buffered saline; AST, aspartate aminotransferase; ALT, alanine aminotrasferase; ApoB, apolipoprotein B; ACSL, acyl-CoA synthetase; VLDL, very low density lipoprotein.

0168-8278/$36.00 © 2009 European Association for the Study of the Liver. Published by Elsevier B.V. All rights reserved.
doi:10.1016/j.jhep.2009.01.018

these therapeutic options, ARBs are initially expected to suppress the development of hepatic fibrosis in NASH. Hepatic stellate cell (HSC), which is a major fibrogenic cell type in the liver and also contributes to hepatic inflammation through induction of cytokines, expresses AT1R, and blockade of Ang II signaling markedly attenuates hepatic inflammation and fibrosis in experimental models of chronic liver fibrosis [8,9]. A clinical report has also demonstrated that losartan, an ARB, improved hepatic necroinflammation and fibrosis in NASH patients [10].

In addition to anti-fibrotic/inflammatory effect, emerging data have suggested that ARBs improve glucose and lipid metabolism. In a large clinical trial, losartan substantially lowered the risk for type 2 diabetes compared with other antihypertensive therapies [11]. An animal study using obese Zucker rats has also demonstrated that high dose of irbesartan improved insulin sensitivity [12]. More recently, it has been shown that telmisartan, unlike other ARBs improved the development of hepatic steatosis in animal models [7,13,14]. These metabolic effects of ARBs might be explained in part by the *in vitro* study, in which a distinct subtype of ARBs induced transcriptional activities of peroxisome proliferator-activated receptor (PPAR) γ, independent of their AT1R blocking actions [15,16]. However, it is noteworthy that PPARγ-activating potency by ARBs appears rather modest as determined by transcription reporter assays, with median effective concentration (EC_{50}) of telmisartan, the most potent PPARγ activator among ARBs, 5.02 μmol/L compared to 0.2 μmol/L of pioglitazone, a full agonist of PPARγ [15,16]. Interestingly, treatment with olmesartan, which has no impact on PPARγ activation, has been proved to attenuate the development of hepatic steatosis, suggesting the possibility that the blockade of AT1R itself might contribute to hepatic lipid homeostasis [17]. To further investigate the direct role for AT1R in hepatic steatosis, we applied two different approaches: (1) animal model of steatohepatitis using mice lacking AT1aR ($AT1a^{-/-}$), which is the only Ang II receptor subtype expressed in rodent liver, and (2) *in vitro* cellular steatosis model in which gene silencing by RNA interference targeting AT1R was performed [18]. Our data demonstrated reduced lipid accumulation in the absence of AT1R with significant induction of PPARα. Apart from PPARγ modulating action of ARBs, these data support the potential efficacy of AT1R blockade in the treatment of NAFLD/NASH.

2. Materials and methods

2.1. Animal

$AT1a^{-/-}$ mice were provided by Mitsubishi Tanabe Pharma (Osaka, Japan) and C57BL/6 mice were obtained from Charles River Laboratories (Yokohama, Japan) [19]. Both strains of the mice have the same genetic background. The mice were housed in a standard 12 h light/dark cycle facility, and fed either standard chow diet or methionine–choline deficient (MCD) diet (Oriental Yeast Co., Tokyo, Japan) for 8 weeks with free access to drinking water. Male mice at 6–8 weeks of age were used in this study, and all animal procedures were performed according to the guidelines of Institute of Laboratory Animal Science, Hiroshima University.

2.2. Histological examination

Liver samples were fixed in 4% formaldehyde solution, embedded in paraffin, and cut into 5 μm-thick sections. Staining for hematoxylin and eosin (H-E) or Azan-Mallory was carried out with standard techniques.

2.3. Analytical techniques

Serum triglyceride (TG) concentration was determined enzymatically using a Triglyceride E-test (Wako Chemicals, Osaka, Japan). To quantify hepatic TG content, hepatic lipid was extracted as previously described by Bligh and Dyer and subjected to the same procedure as serum assay followed by the standardization of protein concentrations [20]. Hepatic thiobarbituric acid-reactive substances (TBARS) levels were quantified using an OXI-TEK TBARS Assay Kit (Zeprometrix Corporation, New York) with protein standardization. Serum TBARS levels were assayed using the same kit. β-Hydroxybutyrate was assayed using an assay kit (BioVision, Mountain View, CA). The activities of serum transaminases were determined enzymatically.

2.4. Cell culture and gene silencing by small interfering RNA (siRNA)

HepG2 cells (human hepatoma cell line) were cultured in Dulbecco's modified Eagle's medium supplemented with 10% (v/v) fetal bovine serum. For gene silencing, two different sequences of small interfering RNA (siRNA) targeting human AT1R were purchased from Sigma–Aldrich (siRNA ID: SASI_Hs01_00206672, SASI_Hs02_00206672). Cells were transfected using Lipofectamine RNAiMAX (Invitrogen) in 6-well plates containing 2.5×10^5 cells in each well with 10 nM of siRNA duplex. siPerfect Negative Controls (Sigma–Aldrich) was utilized as a negative control siRNA. In the preliminary experiment, siRNA duplex of SASI_Hs02_00206672 effectively knocked down AT1R expression compared to SASI_Hs01_00206672, and this was used for the following experiments. After 24 and 48 h of transfection, cells were subjected to gene quantification by real-time PCR and *in vitro* steatosis experiment, respectively.

2.5. In vitro model of cellular steatosis

Palmitic acid (C16:0) and oleic acid (C18:1) (Sigma, St. Louis, MO) were dissolved in isopropanol to obtain 20 or 40 mM stock mixture solution (2:1 oleate: palmitate), and the concentration of vehicle was 1% in final incubations [21]. Telmisartan (provided by Boehringer Ingelheim, Germany) was resolved in dimethyl sulfoxide (DMSO) to obtain 10 mM stock solution. To investigate the effect of telmisartan on cellular steatosis, cells were exposed to 200 or 400 μM of free fatty acids (FFAs) mixture with or without 2 h preincubation of 10 μM telmisartan. To assess the influence of AT1R knockdown on cellular steatosis, cells were treated with FFAs after 48 h of siRNA transfection. Following 24 h of incubation with FFAs, cells were subjected to determination of cellular lipid content by Nile Red assay and β-hydroxybutyrate levels in the media.

2.6. Nile Red assay

The lipid content in cultured cells was quantified fluorometrically using Nile Red, a vital lipophilic dye as previously described [22].

Briefly, cell monolayers were washed twice with phosphate buffered saline (PBS) followed by fixation with 4% formaldehyde solution for 15 min, and washed with PBS twice again. Cells were stained for 30 min with Nile Red solution at a final concentration of 200 μg/ml in PBS. Monolayers were washed thereafter with PBS and measured fluorometorically (excitation; 488 nm. emission; 550 nm) [23].

2.7. Quantitative real-time PCR

Total RNA was isolated using RNeasy Mini Kit (Qiagen, Germany). cDNA was synthesized from 1 μg of total RNA with GeneAmp Gold RNA PCR Core Kit (Applied Biosystems, Foster City, CA). To quantify AT1R mRNA expression in human heart and kidney, PCR Ready First Strand cDNA (BioChain, Hayward, CA) was utilized. Specific primers except AT1R from PrimerBank, a public resource for PCR primers (http://pga.mgh.harvard.edu/primerbank/, ID: 14043066) were designed using Primer3 (http://frodo.wi.mit.edu) with nucleotide sequences from GenBank™ as listed in Table 1. Real-time PCR was carried out with Lightcycler 1.5 system using Lightcycler FastStart DNA Master plus SYBR Green I (Roche Applied Science). The relative expression levels were calculated with the formula $2^{-\Delta C_t}$, where ΔC_t is the difference in threshold cycle (C_t) values between target gene and ribosomal protein S18 as a control.

2.8. Western blot analysis for AT1R

Fifty microgram of protein prepared from HepG2 cells using RIPA buffer supplemented with protease inhibitors (Roche Diagnostics), as well as Total Protein-Human Adult Normal Tissues (Biochain, Hayward, CA) were fractionated by SDS–PAGE and subjected to Western blot analysis using rabbit polyclonal antibodies against human AT1R (N-10) (Santa Cruz Biotechnology, Santa Cruz, CA). The blots were visualized by enhanced chemiluminescence.

2.9. Statistical analysis

The data are expressed as the means ± SE. The statistical analysis was performed using Student's t test, and differences were considered statistically significant for a two-tailed $p < 0.05$.

3. Results

3.1. Mice lacking AT1R are resistant to steatohepatitis

MCD diet has been reported to cause steatohepatitis which represents most of histological features of human NASH [24,25]. As shown in Fig. 1A, histological analysis of the livers demonstrated that MCD diet for 8 weeks resulted in apparent steatosis with inflammatory cell infiltration mainly in portal area in wild-type (WT) mice. However, in contrast to WT mice, $AT1a^{-/-}$ mice displayed no significant changes in the liver (Fig. 1A, right panel). Azan-Mallory staining of the liver from WT mice revealed mild pericellular fibrosis, which was absent in $AT1a^{-/-}$ mice (Fig. 1A, lower panels). In accordance with these histological observations, hepatic TG content increased by 3-fold in WT and remained no significant 1.5-fold increase in $AT1a^{-/-}$ mice following 8 weeks of MCD diet (Fig. 1B, left panel). Serum TG level following MCD diet was reduced in both genetic groups with more drastic change in WT mice (Fig. 1B, right panel). The substantial changes in hepatic TG content suggested the possibility that the expression of PPARα, a central player in hepatic lipid metabolism, might be influenced by AT1aR expression. This was assessed by quantitative real-time PCR. While MCD diet did not affect hepatic PPARα expression in both genetic strains, absence of AT1aR was associated with significant 3-fold increase in PPARα mRNA in chow diet-fed mice (Fig. 1C). Since PPARα mediates hepatic expression of genes regulating lipid oxidation, we next assessed serum level of β-hydroxybutyrate, an end product of hepatic fatty acid oxidation. Fig. 1D demonstrates 3-fold increase in serum β-hydroxybutyrate in $AT1a^{-/-}$ mice compared to WT mice following MCD diet. This might be a potential explanation for reduced hepatic lipid accumulation in $AT1a^{-/-}$ mice.

3.2. Lack of AT1R ameliorates liver injury

As shown in Fig. 2, there were no differences in aspartate aminotransferase (AST) and alanine aminotrasferase (ALT) levels between WT and $AT1a^{-/-}$ mice when fed chow diet. MCD diet caused significant increase in AST and ALT levels in WT mice, whereas there was no significant increase of these liver enzymes in $AT1a^{-/-}$ mice.

Table 1
Primer used for quantitative real-time PCR.

Gene	Forward	Reverse	GenBank Accession No.
mPPARα	tgcaaacttggacttgaacg	tgatgtcacagaacggcttc	BC016892
AT1	atccaagatgattgtcccaaagc	gcccatagtggcaaagtcagtaa	
PPARα	cagtggagcattgaacatcg	gttgtgtgacatcccgacag	NM_001001928
ApoB100	agccttgctgaagaaaacca	atgcccctcttgatgttcag	M14162
ASCL1	ccagaagggcttcaagactg	gccttctctggcttgtcaac	NM_001995
RPS18	atagcctttgccatcactgc	ggacctggctgtattttcca	NM_022551
PPARγ	atcaaagtggagcctgcatc	acccttgcatccttcacaag	NM_138711
PPARβ(δ)	ctatccgttttggtcggatg	cgatgtcgtggatcacaaag	NM_006238

mPPARα, mouse peroxisome proliferator-activated receptor α; AT1, angiotensin II type I receptor; PPAR, human PPAR; ApoB100, apolipoprotein B-100; ACSL1, acyl-CoA synthetase long-chain family member 1; RPS18, ribosomal protein S18.

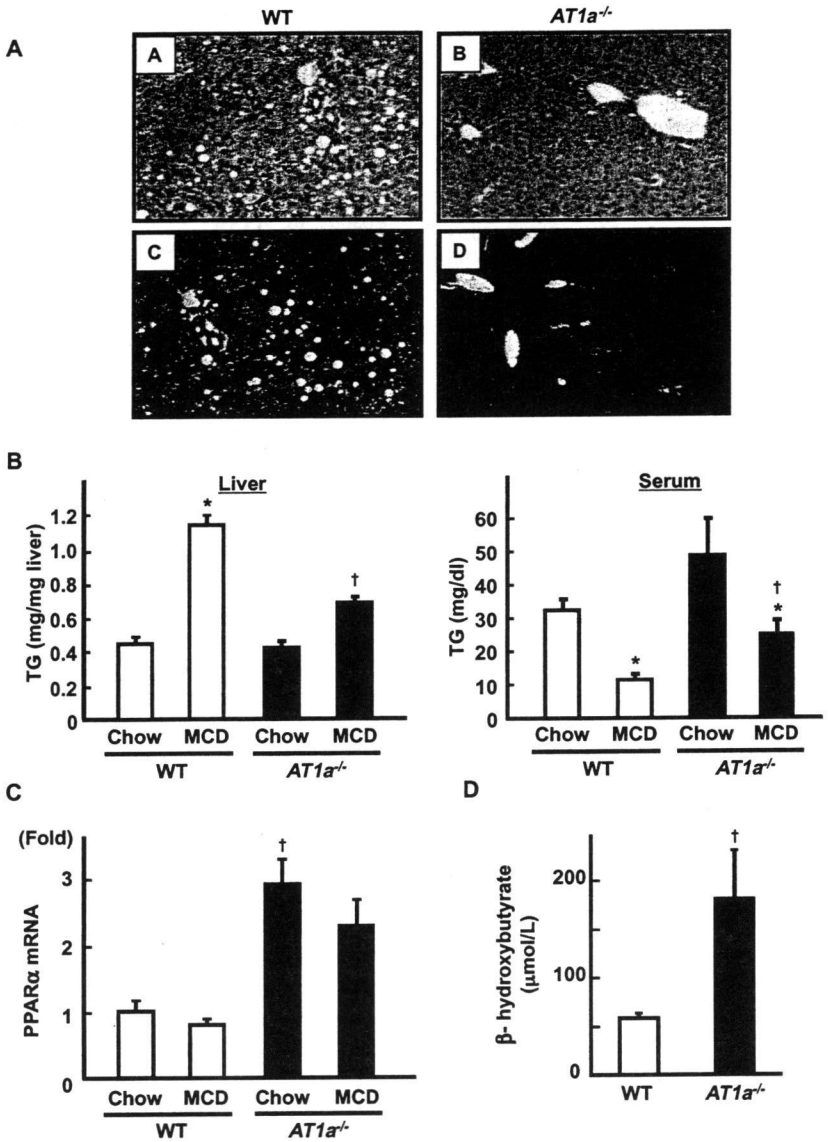

Fig. 1. The absence of AT1aR expression attenuates the development of MCD diet-induced hepatic steatosis in mice. (A) Liver sections from MCD diet-fed WT (A and C) and $AT1a^{-/-}$ mice (B and D) were processed for haematoxylin & eosin (HE) (upper panels) or Azan-Mallory staining (lower panels). Hepatic steatosis as well as fibrosis are evident only in WT mice (original magnification 100×). (B) TG concentrations in liver (left panel) and serum (right panel) obtained from WT (open bars) and $AT1a^{-/-}$ (closed bars) mice (n = 6/each group) were determined after feeding either normal chow or MCD diet. (C) Hepatic PPARα mRNA expression was quantified (n = 5/each group) by quantitative real-time PCR. (D) The serum level of β-hydroxybutyrate in WT (n = 5) and $AT1a^{-/-}$(n = 6) mice fed MCD diet was determined. $^{*}p < 0.05$, chow-fed vs. MCD diet-fed mice. $^{\dagger}p < 0.05$, WT vs. $AT1a^{-/-}$ mice. [This figure appears in colour on the web.]

3.3. Influence of AT1R expression on oxidative stress

Since lipid peroxidation product plays an important role as a "2nd hit" in the pathogenesis of NASH, we next examined serum and hepatic levels of TBARS [26]. Fig. 3 demonstrates marked increase in TBARS levels in serum and liver of WT mice following MCD diet. In contrast, $AT1a^{-/-}$ mice showed no significant changes in TBARS levels, which presumably reflected the reduction of liver injury as demonstrated in AST and ALT levels.

3.4. Expression of AT1R in the liver and HepG2 cells

To further explore the protective effect of AT1R blockade in hepatic steatosis observed in animal model, we performed *in vitro* studies using HepG2 cells. We first ascertained AT1R expression in HepG2 cells comparing

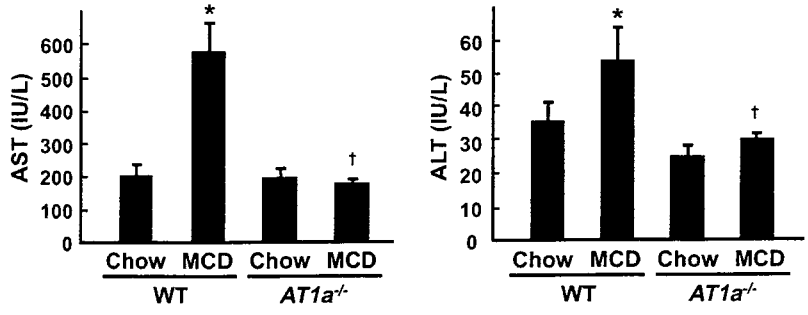

Fig. 2. Diminished hepatic injury following 8 weeks of MCD diet in the absence of AT1aR. AST and ALT levels were determined in WT (open bars) and $AT1a^{-/-}$ (closed bars) mice fed either normal chow or MCD diet for 8 weeks (n = 6/each group). $^{*}p < 0.05$, chow-fed vs. MCD diet-fed mice. $^{\dagger}p < 0.05$, WT vs. $AT1a^{-/-}$ mice.

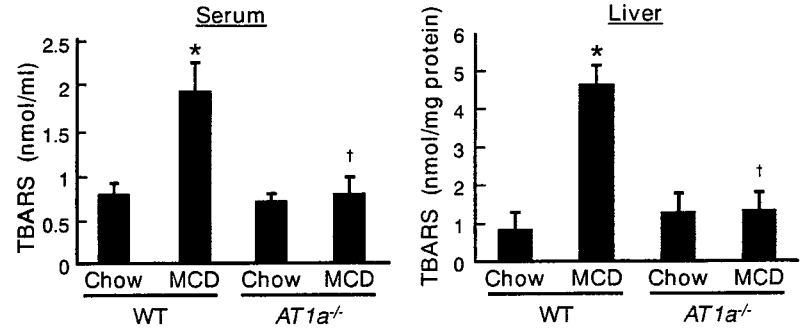

Fig. 3. Influence of AT1aR expression on TBARS levels in serum and liver. TBARS levels were assayed in serum (left panel) and liver (right panel) from WT (open bars) and $AT1a^{-/-}$ (closed bars) mice after feeding either normal chow or MCD diet (n = 6/each group). $^{*}p < 0.05$, chow-fed vs. MCD diet-fed mice. $^{\dagger}p < 0.05$, WT vs. $AT1a^{-/-}$ mice.

that of heart, kidney, and liver tissues, which are known to express functional AT1R. As displayed in Fig. 4, Western blot analysis revealed AT1R protein expression in HepG2 cells, supporting the previous *in vivo* binding assay of Ang II that detected a homogeneous signal pattern throughout the liver parenchyma [27]. Although the quantities of loaded protein were the same among samples, the band intensity in HepG2 appeared to be weaker compared to whole liver homogenate, which comprises non-parenchymal liver cells such as hepatic stellate cells and Kupffer cells. However, real-time PCR demonstrated similar level of AT1R in HepG2 as compared to kidney (Fig. 4, right panel).

3.5. AT1R blockade reduces lipid accumulation in hepatocellular in vitro model

To examine whether AT1R expression in HepG2 was functional, we utilized *in vitro* model of steatosis in which HepG2 cells were treated with FFAs mixture with or without 10 μM of telmisartan. As shown in Fig. 5A, Nile Red assay quantified 4- to 5-fold increase in cellular

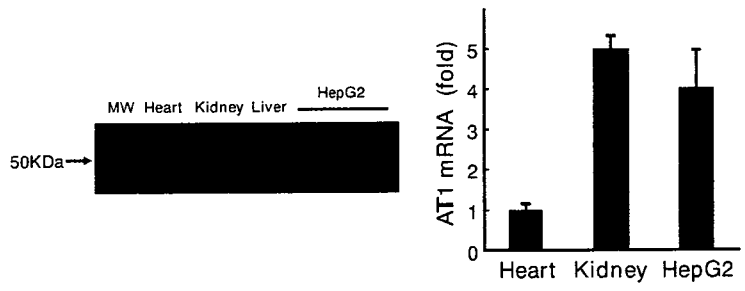

Fig. 4. Expressions of AT1R in the liver and HepG2 cells. Western blots of AT1R protein expression in homogenates from human liver and HepG2 cells by comparison with heart and kidney as positive tissues for AT1R expression (50 KDa) (left panel). Quantitative real-time PCR analysis for AT1R in HepG2 (right panel). Results represent from at least three independent experiments.

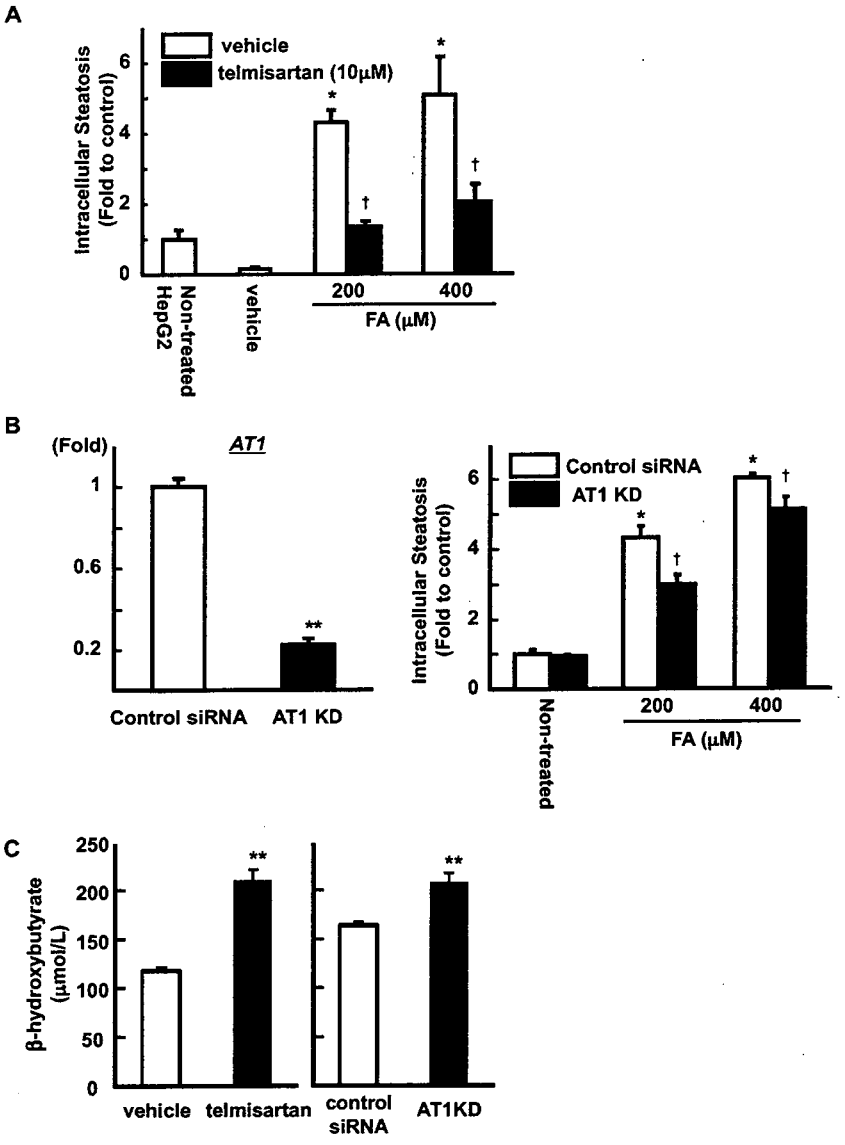

Fig. 5. AT1R blockade attenuates cellular steatosis following fatty acids overload. (A) Influence of telmisartan on intracellular steatosis induced by free fatty acids (FFAs) overload (2:1 oleate: palmitate) (n = 6/each group). (B) Effect of siRNA targeting AT1R on *AT1* mRNA expression (left panel) and influence of AT1 knockdown (KD) on cellular steatosis induced by FFAs overload (2:1 oleate: palmitate, right panel) (n = 6/each group). (C) Influence of AT1R blockade on β-hydroxybutyrate levels in media (n = 6/each group). $^{**}p < 0.005$, vs. control siRNA. $^{*}p < 0.05$, vs. non-treated groups. $^{\dagger}p < 0.05$, AT1R blockade (either by telmisartan or AT1 knockdown) vs. control (either vehicle or control siRNA) HepG2.

lipid accumulation when cells were treated with FFAs for 24 h in the absence of telmisartan. These changes were markedly attenuated by the presence of telmisartan by 60–70%. To exclude the possibility that these anti-steatotic effects might be attributable to pharmacological property of telmisartan, we investigated the influence of AT1R knockdown using siRNA in the same experimental model. As shown in Fig. 5B, transfection of HepG2 cells with siRNA targeting AT1R successfully depleted its mRNA expression by 80% when compared to control siRNA. This siRNA knockdown of AT1R resulted in significant 15–30% decrease in cellular lipid deposition following FFAs exposure (Fig. 5B, right panel). Compared to the treatment of telmisartan, the influence of AT1R knockdown appeared modest. This might be because siRNA suppression of AT1R was not sufficient to elicit complete inhibition of the AT1R signaling pathway. In connection with the observed ketogenesis in $AT1a^{-/-}$ mice, we examined β-hydroxybutyrate levels in the culture media. Under the condition

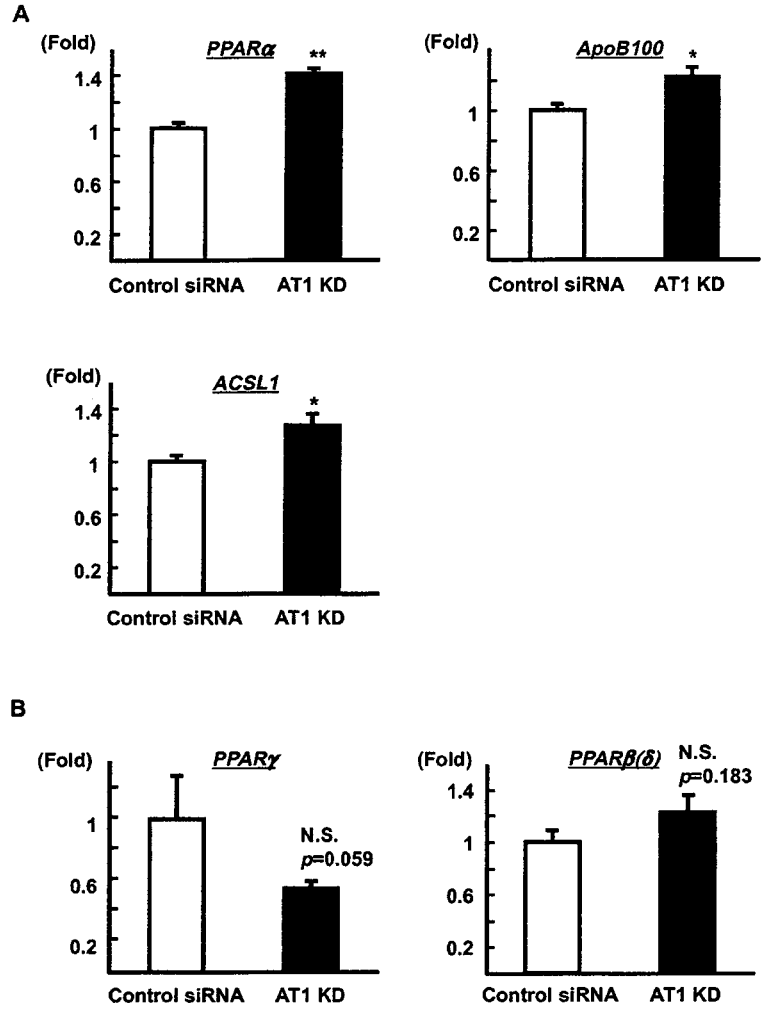

Fig. 6. Influence of AT1R knockdown on the expression of PPARα target genes (A) and the other PPAR isoforms (B). Real-time PCR quantified the expression of genes regulated by PPARα as well as of the other PPAR isoforms, PPARγ and PPARβ(δ) in HepG2 cells transfected with either siRNA targeting AT1R ($n = 6$) or negative control siRNA ($n = 6$). $^{*}p < 0.05$, vs. control siRNA. $^{**}p < 0.005$, vs. control siRNA. NS, not statistically significant.

of 200 μM of FFAs overload, the treatment of telmisartan as well as AT1R knockdown significantly increased β-hydroxybutyrate levels (Fig. 5C).

3.6. AT1R knockdown induces PPARa and its target genes

The observation that hepatic PPARα expression was up-regulated in *AT1a*$^{-/-}$ mice suggests the possible link between AT1R signaling and PPARα expression. In this setting, our working hypothesis was that AT1R down-regulation might in turn influence the hepatocellular expressions of PPARα and its target genes. As shown in Fig. 6A, transient AT1R silencing by siRNA resulted in significant up-regulation of *PPARα* by 41%. In addition, PPARα target genes, acyl-CoA synthetase 1 (*ACSL1*) and apolipoprotein B (*ApoB*) 100 were also induced by 27% and 21%, respectively. These data exclude the possibility that PPARα up-regulation in *AT1a*$^{-/-}$ mice might be resulted from chronic adaptation to the absence of AT1R. To exclude the possible contribution of the other PPAR isoforms in hepatocellular steatosis, the expression of PPARγ and PPARβ(δ) were assessed by real-time PCR, which resulted in no significant changes following AT1R depletion (Fig. 6B).

4. Discussion

The present study indicates a major role for AT1R in hepatic steatosis by providing a precise genetic approach. Homozygous disruption of AT1R in mice resulted in marked reduction of hepatic lipid accumulation as determined morphologically and by hepatic TG

content. Recent studies have demonstrated that ARBs improve insulin resistance and hyperinsulinemia. Because the improvement of insulin resistance leads to reduction of FFAs flux to the liver together with increased uptake and storage of FFAs in adipose tissue, ARBs are expected to reduce hepatic steatosis. However, the effect of ARBs on hepatic steatosis is still controversial [7,14,17,28–30]. These conflicting findings might be explained by differences in selective PPARγ modulating properties of ARBs [15,16], or attributed to differences in the dose and length of ARBs supplementation as well as potential differences in the mechanisms of steatosis in the different experimental models. Our data reinforces the theory that blockade of AT1R, unrelated to pharmacological properties of ARBs, ameliorates the development of hepatic steatosis.

The pathophysiology of NASH remains poorly understood, but is often described as "two-hit process" consisting of hepatic TG accumulation (the 1st step) and development of oxidative stress and proinflammatory cytokines (the 2nd step), which leads to hepatocyte injury, inflammation, and fibrosis [26]. Previous reports have demonstrated that pharmacological blockade or gene deletion of renin-angiotensin system (RAS) significantly attenuates hepatic fibrosis in experimental animal models [31,32]. Moreover, Ang II, the effecter peptide for AT1R, has been reported to stimulates an array of fibrogenic actions in activated HSCs through the mediation of reactive oxygen species [33]. More recent data has revealed that angiotensin converting enzyme (ACE) deficient ($ACE^{-/-}$) mice which exhibit reduced levels of Ang II by 70% in plasma and by 85–97% in tissues [34] showed pronounced increase in hepatic gene expression related to lipolysis and fatty acid oxidation, suggesting close link between RAS and hepatic lipid metabolism [35]. Taken together with our finding of the anti-steatotic effect, the blockade of AT1R appears to contribute to wide range of steps and phases in the pathogenesis of NASH.

The up-regulation of PPARα in the liver of $AT1a^{-/-}$ mice is intriguing because PPARα plays a central role in hepatic lipid homeostasis. It is well known that many of the genes encoding enzymes involved in the mitochondrial and peroxisomal fatty acid β-oxidation pathways are regulated by PPARα. To exclude the possibility that adaptation to persistent AT1R absence may induce PPARα expression in mice, we performed *in vitro* siRNA experiments, which confirmed induction of PPARα and its target genes by transient AT1R knockdown. In support of these observations, previous experiments have demonstrated telmisartan-mediated induction of PPARα [36]. Whereas induction of PPARα was observed in $AT1a^{-/-}$ mice, the present study lacks the direct evidence that suppressive effect of AT1R blockade on hepatic steatosis is mediated by PPARα. In this connection, we examined β-hydroxybutyrate levels since it is documented that PPARα activation leads to stimulation of ketogenesis [37,38]. This yielded marked increase in serum β-hydroxybutyrate in $AT1a^{-/-}$ mice. In addition, our *in vitro* experiments demonstrated significant increase in β-hydroxybutyrate in the culture media in response to AT1R blockade. These findings support the detected changes in gene expressions of PPARα and ACSL1 following AT1R deletion. Although it remains controversial whether the blockade of AT1R directly stimulates PPARα, up-regulation of PPARα likely increases the sensitivity to agonist and thus clinical usage of ARBs together with PPARα ligand such as fibrates might have synergistic effects on hepatic lipid metabolism.

A potential limitation of the present study is the use of MCD dietary animal model. Although this model develops steatohepatitis morphologically similar to human NASH with an increase in oxidative stress and has been widely used for the study of NASH, absence of insulin resistance has been reported [24,25,39,40]. Since insulin resistance is considered to be pivotal in the development of NASH, this model might not entirely reflect the natural course and the etiological background of human NASH [41,42]. Some other potential dietary models include *ad libitum* feeding of the high fat diet, which develops obesity and insulin resistance but not noticeable steatohepatitis [43]. Additionally, intragastric overfeeding of high fat diet induces NASH pathology, but some of the biological changes observed in the liver did not mimic human NASH [44]. Altogether, the study of pathophysiological process of NASH is limited by the lack of suitable experimental animal models [45]. Interestingly, the effect of olmesartan has been investigated in a genetically diabetic rat fed MCD diet [30]. In contrast to our findings, olmesartan reduced hepatic steatosis only in diabetic but not in control rats. In the present study, MCD diet caused increase in hepatic TG content associated with decrease in serum TG level, suggesting that impaired TG secretion from liver might contribute to hepatic steatosis. These changes were blunted in the absence of AT1R, implying improvement of TG secretion in $AT1a^{-/-}$ mice. This might be in part explained by the observation of *in vitro* experiment that AT1 knockdown induced ApoB which is requisite for the formation of very low density lipoprotein (VLDL).

In the present study, human hepatoma cell line HepG2 instead of rodent primary hepatocytes was utilized for *in vitro* model of cellular steatosis. This was based on the previous report that human primary hepatocytes and HepG2 cells reached similar levels of intracellular lipid accumulation close to that determined in hepatocytes from human steatosis liver [23]. In addition, the observed up-regulation of hepatic PPARα in $AT1a^{-/-}$ mice led to the speculation that PPARα might play a role in the anti-steatotic effect of AT1 blockade.

Because hepatic expression of PPARα and the sensitivity to it notably differ among species [46], human-derived cell line was applied.

In conclusion, mice lacking AT1R are resistant to the development of hepatic steatosis with up-regulation of PPARα in MCD diet-induced steatohepatitis model. Accordingly, the levels of TBARS, a marker of oxidative stress, as well as aminotransferases, indicators of liver damage were significantly attenuated in *AT1a*$^{-/-}$ mice. In addition, an *in vitro* experiment of hepatocellular steatosis revealed that blockade of AT1R by telmisartan and specific siRNA knockdown markedly decreased cellular lipid accumulation. Up-regulation of PPARα was also confirmed by transient AT1R knockdown. These data provide strong evidence that, in addition to pharmacological effect of ARBs on PPARγ activation, AT1R signaling is involved in hepatic lipid metabolism.

Acknowledgements

The authors thank Dr. Naseem Gaur for helpful discussion. This work was supported by a Grant-in-aid from the Ministry of Health, Labor and Welfare of Japan to S. Tazuma. This work was carried out in part at the Analysis Center of Life Science, Hiroshima University.

References

[1] Belfort R, Harrison SA, Brown K, Darland C, Finch J, Hardies J, et al. A placebo-controlled trial of pioglitazone in subjects with non-alcoholic steatohepatitis. N Engl J Med 2006;355:2297–2307.
[2] Promrat K, Lutchman G, Uwaifo GI, Freedman RJ, Soza A, Heller T, et al. A pilot study of pioglitazone treatment for non-alcoholic steatohepatitis. Hepatology 2004;39:188–196.
[3] Marchesini G, Brizi M, Bianchi G, Tomassetti S, Zoli M, Melchionda N. Metformin in non-alcoholic steatohepatitis. Lancet 2001;358:893–894.
[4] Antonopoulos S, Mikros S, Mylonopoulou M, Kokkoris S, Giannoulis G. Rosuvastatin as a novel treatment of non-alcoholic fatty liver disease in hyperlipidemic patients. Atherosclerosis 2006;184:233–234.
[5] Basaranoglu M, Acbay O, Sonsuz A. A controlled trial of gemfibrozil in the treatment of patients with non-alcoholic steatohepatitis. J Hepatol 1999;31:384.
[6] Jin H, Yamamoto N, Uchida K, Terai S, Sakaida I. Telmisartan prevents hepatic fibrosis and enzyme-altered lesions in liver cirrhosis rat induced by a choline-deficient L-amino acid-defined diet. Biochem Biophys Res Commun 2007;364:801–807.
[7] Fujita K, Yoneda M, Wada K, Mawatari H, Takahashi H, Kirikoshi H, et al. Telmisartan, an angiotensin II type 1 receptor blocker, controls progress of non-alcoholic steatohepatitis in rats. Dig Dis Sci 2007;52:3455–3464.
[8] Bataller R, Gines P, Nicolas JM, Gorbig MN, Garcia-Ramallo E, Gasull X, et al. Angiotensin II induces contraction and proliferation of human hepatic stellate cells. Gastroenterology 2000;118:1149–1156.
[9] Kanno K, Tazuma S, Nishioka T, Hyogo H, Chayama K. Angiotensin II participates in hepatic inflammation and fibrosis through MCP-1 expression. Dig Dis Sci 2005;50:942–948.
[10] Yokohama S, Yoneda M, Haneda M, Okamoto S, Okada M, Aso K, et al. Therapeutic efficacy of an angiotensin II receptor antagonist in patients with non-alcoholic steatohepatitis. Hepatology 2004;40:1222–1225.
[11] Dahlof B, Devereux RB, Kjeldsen SE, Julius S, Beevers G, de Faire U, et al. Cardiovascular morbidity and mortality in the Losartan Intervention For Endpoint reduction in hypertension study (LIFE): a randomised trial against atenolol. Lancet 2002;359:995–1003.
[12] Henriksen EJ, Jacob S, Kinnick TR, Teachey MK, Krekler M. Selective angiotensin II receptor antagonism reduces insulin resistance in obese Zucker rats. Hypertension 2001;38:884–890.
[13] Sugimoto K, Kazdova L, Qi NR, Hyakukoku M, Kren V, Simakova M, et al. Telmisartan increases fatty acid oxidation in skeletal muscle through a peroxisome proliferator-activated receptor-gamma dependent pathway. J Hypertens 2008;26:1209–1215.
[14] Ibanez P, Solis N, Pizarro M, Aguayo G, Duarte I, Miquel JF, et al. Effect of losartan on early liver fibrosis development in a rat model of non-alcoholic steatohepatitis. J Gastroenterol Hepatol 2007;22:846–851.
[15] Benson SC, Pershadsingh HA, Ho CI, Chittiboyina A, Desai P, Pravenec M, et al. Identification of telmisartan as a unique angiotensin II receptor antagonist with selective PPARgamma-modulating activity. Hypertension 2004;43:993–1002.
[16] Schupp M, Janke J, Clasen R, Unger T, Kintscher U. Angiotensin type 1 receptor blockers induce peroxisome proliferator-activated receptor-gamma activity. Circulation 2004;109:2054–2057.
[17] Hirose A, Ono M, Saibara T, Nozaki Y, Masuda K, Yoshioka A, et al. Angiotensin II type 1 receptor blocker inhibits fibrosis in rat non-alcoholic steatohepatitis. Hepatology 2007;45:1375–1381.
[18] Burson JM, Aguilera G, Gross KW, Sigmund CD. Differential expression of angiotensin receptor 1A and 1B in mouse. Am J Physiol 1994;267:E260–E267.
[19] Sugaya T, Nishimatsu S, Tanimoto K, Takimoto E, Yamagishi T, Imamura K, et al. Angiotensin II type 1a receptor-deficient mice with hypotension and hyperreninemia. J Biol Chem 1995;270:18719–18722.
[20] Bligh EG, Dyer WJ. A rapid method of total lipid extraction and purification. Can J Biochem Physiol 1959;37:911–917.
[21] Malhi H, Bronk SF, Werneburg NW, Gores GJ. Free fatty acids induce JNK-dependent hepatocyte lipoapoptosis. J Biol Chem 2006;281:12093–12101.
[22] Greenspan P, Fowler SD. Spectrofluorometric studies of the lipid probe, nile red. J Lipid Res 1985;26:781–789.
[23] Gomez-Lechon MJ, Donato MT, Martinez-Romero A, Jimenez N, Castell JV, O'Connor JE. A human hepatocellular in vitro model to investigate steatosis. Chem Biol Interact 2007;165:106–116.
[24] Tomita K, Oike Y, Teratani T, Taguchi T, Noguchi M, Suzuki T, et al. Hepatic AdipoR2 signaling plays a protective role against progression of non-alcoholic steatohepatitis in mice. Hepatology 2008;48:458–473.
[25] Igolnikov AC, Green RM. Mice heterozygous for the Mdr2 gene demonstrate decreased PEMT activity and diminished steatohepatitis on the MCD diet. J Hepatol 2006;44:586–592.
[26] Day CP, James OF. Steatohepatitis: a tale of two "hits? Gastroenterology 1998;114:842–845.
[27] Paizis G, Cooper ME, Schembri JM, Tikellis C, Burrell LM, Angus PW. Up-regulation of components of the renin-angiotensin system in the bile duct-ligated rat liver. Gastroenterology 2002;123:1667–1676.
[28] Ran J, Hirano T, Adachi M. Angiotensin II infusion increases hepatic triglyceride production via its type 2 receptor in rats. J Hypertens 2005;23:1525–1530.
[29] Sugimoto K, Qi NR, Kazdova L, Pravenec M, Ogihara T, Kurtz TW. Telmisartan but not valsartan increases caloric expenditure

and protects against weight gain and hepatic steatosis. Hypertension 2006;47:1003–1009.
[30] Kurita S, Takamura T, Ota T, Matsuzawa-Nagata N, Kita Y, Uno M, et al. Olmesartan ameliorates a dietary rat model of non-alcoholic steatohepatitis through its pleiotropic effects. Eur J Pharmacol 2008;588:316–324.
[31] Yoshiji H, Kuriyama S, Yoshii J, Ikenaka Y, Noguchi R, Nakatani T, et al. Angiotensin-II type 1 receptor interaction is a major regulator for liver fibrosis development in rats. Hepatology 2001;34:745–750.
[32] Kanno K, Tazuma S, Chayama K. AT1A-deficient mice show less severe progression of liver fibrosis induced by CCl(4). Biochem Biophys Res Commun 2003;308:177–183.
[33] Bataller R, Schwabe RF, Choi YH, Yang L, Paik YH, Lindquist J, et al. NADPH oxidase signal transduces angiotensin II in hepatic stellate cells and is critical in hepatic fibrosis. J Clin Invest 2003;112:1383–1394.
[34] Campbell DJ, Alexiou T, Xiao HD, Fuchs S, McKinley MJ, Corvol P, et al. Effect of reduced angiotensin-converting enzyme gene expression and angiotensin-converting enzyme inhibition on angiotensin and bradykinin peptide levels in mice. Hypertension 2004;43:854–859.
[35] Jayasooriya AP, Mathai ML, Walker LL, Begg DP, Denton DA, Cameron-Smith D, et al. Mice lacking angiotensin-converting enzyme have increased energy expenditure, with reduced fat mass and improved glucose clearance. Proc Natl Acad Sci USA 2008;105:6531–6536.
[36] Clemenz M, Frost N, Schupp M, Caron S, Foryst-Ludwig A, Bohm C, et al. Liver-specific peroxisome proliferator-activated receptor alpha target gene regulation by the angiotensin type 1 receptor blocker telmisartan. Diabetes 2008;57:1405–1413.
[37] Mandard S, Müller M, Kersten S. Peroxisome proliferator-activated receptor alpha target genes. Cell Mol Life Sci 2004;61:393–416.
[38] Luci S, Giemsa B, Kluge H, Eder K. Clofibrate causes an upregulation of PPAR-{alpha} target genes but does not alter expression of SREBP target genes in liver and adipose tissue of pigs. Am J Physiol Regul Integr Comp Physiol 2007;293:R70–R77.
[39] Rinella ME, Green RM. The methionine–choline deficient dietary model of steatohepatitis does not exhibit insulin resistance. J Hepatol 2004;40:47–51.
[40] Vetelainen R, van Vliet A, van Gulik TM. Essential pathogenic and metabolic differences in steatosis induced by choline or methione-choline deficient diets in a rat model. J Gastroenterol Hepatol 2007;22:1526–1533.
[41] Pagano G, Pacini G, Musso G, Gambino R, Mecca F, Depetris N, et al. Non-alcoholic steatohepatitis, insulin resistance, and metabolic syndrome: further evidence for an etiologic association. Hepatology 2002;35:367–372.
[42] Sanyal AJ, Campbell-Sargent C, Mirshahi F, Rizzo WB, Contos MJ, Sterling RK, et al. Nonalcoholic steatohepatitis: association of insulin resistance and mitochondrial abnormalities. Gastroenterology 2001;120:1183–1192.
[43] Collins S, Martin TL, Surwit RS, Robidoux J. Genetic vulnerability to diet-induced obesity in the C57BL/6J mouse: physiological and molecular characteristics. Physiol Behav 2004;81:243–248.
[44] Deng QG, She H, Cheng JH, French SW, Koop DR, Xiong S, et al. Steatohepatitis induced by intragastric overfeeding in mice. Hepatology 2005;42:905–914.
[45] Koteish A, Mae Diehl A. Animal models of steatohepatitis. Best Pract Res Clin Gastroenterol 2002;16:679–690.
[46] Gonzalez FJ, Peters JM, Cattley RC. Mechanism of action of the nongenotoxic peroxisome proliferators: role of the peroxisome proliferator-activator receptor alpha. J Natl Cancer Inst 1998;90:1702–1709.

GASTROENTEROLOGY 2009;137:673–681

Amphipathic DNA Polymers Inhibit Hepatitis C Virus Infection by Blocking Viral Entry

TAKUYA MATSUMURA,* ZONGYI HU,* TAKANOBU KATO,* MARLENE DREUX,‡ YONG-YUAN ZHANG,* MICHIO IMAMURA,§ NOBUHIKO HIRAGA,§ JEAN-MARC JUTEAU,‖ FRANCOIS-LOIC COSSET,‡ KAZUAKI CHAYAMA,§ ANDREW VAILLANT,‖ and T. JAKE LIANG*

*Liver Diseases Branch, National Institute of Diabetes and Digestive and Kidney Diseases, National Institutes of Health, Bethesda, Maryland; ‡Universite de Lyon, INSERM U758, and Ecole Normale Superieure de Lyon, Lyon, France; §Department of Medicine and Molecular Science, Division of Frontier Medical Science, Graduate School of Biomedical Sciences, Hiroshima University, Hiroshima, Japan; and ‖REPLICor Inc, Laval, Quebec, Canada

See editorial on page 427.

BACKGROUND & AIMS: Hepatitis C virus (HCV) gains entry into susceptible cells by interacting with cell surface receptor(s). Viral entry is an attractive target for antiviral development because of the highly conserved mechanism. **METHODS:** HCV culture systems were used to study the effects of phosphorothioate oligonucleotides (PS-ONs), as amphipathic DNA polymers (APs), on HCV infection. The in vivo effects of APs were tested in urokinase plasminogen activator (uPA)/severe combined immunodeficient (SCID) mice engrafted with human hepatocytes. **RESULTS:** We show the sequence-independent inhibitory effects of APs on HCV infection. APs were shown to potently inhibit HCV infection at submicromolar concentrations. APs exhibited a size-dependent antiviral activity and were equally active against HCV pseudoparticles of various genotypes. Control phosphodiester oligonucleotide (PO-ON) polymer without the amphipathic structure was inactive. APs had no effect on viral replication in the HCV replicon system or binding of HCV to cells but inhibited viral internalization, indicating that the target of inhibition is at the postbinding, cell entry step. In uPA/SCID mice engrafted with human hepatocytes, APs efficiently blocked de novo HCV infection. **CONCLUSIONS: Our results demonstrate that APs are a novel class of antiviral compounds that hold promise as a drug to inhibit HCV entry.**

Hepatitis C virus (HCV) infects approximately 200 million people worldwide.[1] The majority of HCV-infected patients fails to clear the virus, and many develop chronic liver disease including cirrhosis with a risk of hepatocellular carcinoma. Treatment of chronic hepatitis C is currently based on peginterferon-alfa and ribavirin, which is accompanied by substantial adverse effects and is only effective in approximately half of the patients.[2,3] In addition to other viral targets, viral entry is an attractive target for antiviral development because of the potentially conserved mechanism of viral entry.[4] Although several candidate receptors for HCV have been identified,[5–10] the mechanism of HCV entry still remains largely unknown. Previous reports have indicated a pH dependency for entry of HCV pseudoparticles (HCVpp) as well as cell culture-generated HCV (HCVcc), suggesting that HCV enters cells by receptor-mediated endocytosis.[7,11,12] Antiviral compounds targeting the entry step of viral infection have been successfully developed in other viral infections.[13] Recent studies have shown that phosphorothioate oligonucleotides (PS-ONs), as amphipathic DNA polymers (APs), have a sequence-independent antiviral activity against human immunodeficiency virus type 1 (HIV-1) as entry inhibitors.[14] The antiviral effect of APs appears to be specific to the phosphorothioate backbone, which confers an amphipathic structure, because the phosphodiester oligonucleotides (PO-ONs) as nonamphipathic polymers are ineffective.[14]

Materials and Methods

Cell Culture and Oligonucleotide Synthesis

Huh7.5 (provided by Charles Rice), Huh7.5.1 (provided by Francis Chisari), Huh7, and Hep3B cells were maintained at 37°C, 5% CO_2 in Dulbecco's modified Eagle medium, containing 10% fetal bovine serum. All PS-ONs and PO-ONs were synthesized as described previously.[14] Oligonucleotides lacking the phosphorothioate modification (PO-ONs) were synthesized with the addition of 2′-O-methyl ribose modification, which stabilizes oligonucleotides from nuclease degradation.[14] Compounds used in the in vivo experiment were synthesized under good manufacturing practice (GMP) conditions to yield high-purity sodium salts.

Abbreviations used in this paper: APs, amphipathic DNA polymers; HCV, hepatitis C virus; HCVcc, cell culture-generated HCV; HCVpp, HCV pseudoparticles; VSVGpp, vesicular stomatitis virus G protein pseudoparticle; PO-ON, phosphodiester oligonucleotide; PS-ONs, phosphorothioate oligonucleotides.

0016-5085/09/$36.00
doi:10.1053/j.gastro.2009.04.048